QM/MM Study of Dehydro and Dihydro β-Ionone Retinal Analogues in Squid and Bovine Rhodopsins: Implications for Vision in Salamander Rhodopsin

ARTICLE *in* JOURNAL OF THE AMERICAN CHEMICAL SOCIETY · OCTOBER 2010

Impact Factor: 12.11 · DOI: 10.1021/ja105050p · Source: PubMed

3 AUTHORS:

Sekhar ss

24 PUBLICATIONS **391** CITATIONS

SEE PROFILE

Ahmet Altun

Fatih University

47 PUBLICATIONS **1,718** CITATIONS

SEE PROFILE

Keiji Morokuma

Fukui Institute for Fundamental Chemistry

442 PUBLICATIONS **13,805** CITATIONS

SEE PROFILE

Published in final edited form as:
J Am Chem Soc. 2010 November 17; 132(45): 15856–15859. doi:10.1021/ja105050p.

QM/MM Study of Dehydro and Dihydro β-Ionone Retinal Analogues in Squid and Bovine Rhodopsins: Implications for Vision in Salamander Rhodopsin

Sivakumar Sekharan[†], **Ahmet Altun**[†], and **Keiji Morokuma**[†,¶,*]

[†] Cherry L. Emerson Center for Scientific Computation and Department of Chemistry, Emory University, Atlanta, Georgia 30322, USA

[¶] Fukui Institute for Fundamental Chemistry, Kyoto University, 34-4 Takano Nishihiraki-cho, Sakyo, Kyoto 606–8103, Japan

Abstract

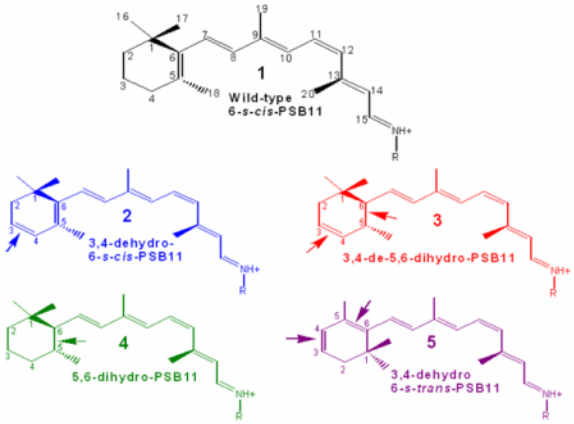

Visual pigment rhodopsin provides a decisive crossing point for interaction between organisms and environment. Naturally occurring visual pigments contain only PSB11 and 3,4-dehydro-PSB11 as chromophores. Therefore, the ability of visual opsin to discriminate between the retinal geometries is investigated by means of QM/MM incorporation of PSB11, 6-*s*-*cis* and 6-*s*-*trans* forms of 3,4-dehydro-PSB11, 3,4-dehydro-5,6-dihydro-PSB11, 5,6-dihydro-PSB11 analogues into squid and bovine rhodopsin environments. The analogue-protein interaction reveals the binding site of squid rhodopsin to be *malleable* and *ductile*, while that of bovine rhodopsin to be *rigid* and *stiff*. On the basis of these studies, a tentative model of salamander rhodopsin binding site is also proposed.

Visual pigment rhodopsin is a G-protein coupled receptor (GPCR) responsible for black/white vision. Invertebrate (squid) and vertebrate (bovine) rhodopsins contain a light absorbing 6-*s*-*cis*-11-*cis*-retinal chromophore covalently bound to the opsin apoprotein via a protonated Schiff-base (PSB11) linkage to the ε-amino group of K305 (squid) and K296 (bovine). The positive charge on the Schiff base nitrogen is counterbalanced with a negatively charged counterion (E180 in squid and E113 in bovine).1⁻3 E180 of squid is ~4

morokuma@emory.edu.

Supporting Information ONIOM (QM/MM)-optimized cartesian coordinates, geometric parameters, excited state properties of the models discussed in this study are available free of charge via the Internet at http://pubs.acs.org.

Å far away from the Schiff-base nitrogen while E113 of bovine is H-bonded to it. We have recently shown theoretically that, E180 and E113 counterions exert almost the same effect of ~100 nm blue-shift on the vertical excitation energy of PSB11 that is almost fully responsible for the spectral shift going from retinal in *vacuo* (610 nm) to those in protein environments: 490 nm (squid)4a,b and 495 nm (bovine).4c

One of the most intriguing and less studied facets of visual pigments is their ability to discriminate between the retinal geometries. In particular, only PSB11 and 3,4-dehydro-PSB11 have been found to act as chromophores in naturally occurring visual pigments.5 Also an analogous molecule, 5,6-dihydro-PSB11 which is similar in all other respects to PSB11 except that the ring is saturated has been found to bind to opsin, but, has not been isolated from retina so far.6 Accumulated evidence from spectral tuning studies on visual pigment using retinal analogues indicate that, a) tiger salamander selects 6-*s*-*cis*- form of 3,4-dehydro-PSB11 and absorbs at ~520 nm,7 b) chicken cone iodopsin selects 6-*s*-*trans*-form of PSB11 to absorb at 562 nm,8 c) deep red cone pigments select 6-*s*-*trans*-geometry that achieves a significant red shift and also enhances its stability within the binding pocket, 9 d) 3,4-dehydro-5,6-dihydro-PSB11 and 5,6-dihydro-PSB11 absorb at ~460 nm and behave as a five-double bonded chromophore.6b Interestingly, dihydro retinals have also been used to characterize the structure of bacterio-,10 sensory-10, and halorhodopsin11 and has been recently shown to even outperform the native pigment in conferring visual photosensitivity. 12

In this study, we have attempted to computationally incorporate 3,4-dehydro-6-*s*-*cis*-(**2**), 3,4-dehydro-5,6-dihydro-(**3**), 5,6-dihydro-(**4**) and 3,4-dehydro-6-*s*-*trans*-(**5**) analogues of PSB11 (see Scheme 1) into bovine and squid rhodopsin binding sites to not only compare and contrast the calculated photophysical properties with that of the native pigment (**1**), but to also gain insights into the evolutionary elasticity of visual rhodopsins. In particular, the aim of the study is five-fold; (i) to document the effect of ring modifications on retinal geometry, (ii) to characterize the general architecture of bovine and squid rhodopsin binding sites, (iii) to identify the origin of spectral tuning mechanism in dehydro and dihydro rhodopsins, (iv) to examine the hypothesis that, optical activity of visual pigments can be manipulated by extension or contraction of the polyene chain,6b and finally, (v) to predict the structure of salamander rhodopsin that contains 3,4-dehydro-6-*s*-*cis*-PSB11 (**2**). As we have chosen retinal analogues that are known to form bleachable visual pigments,13 the calculations are susceptible for further experimental verifications.

To begin with, the QM/MM optimized structure of wild-type squid and bovine rhodopsins are taken from refs. 4a and 4c. By taking the six-double bonded wild-type PSB11 (**1**) as template, an additional double bond is introduced at C3—C4 position to give the seven-double bonded 3,4-dehydro PSB11 (**2**). Subsequent saturation at C5=C6 position gives 3,4-dehydro-5,6-dihydro PSB11 (**3**) and at C3=C4 position (in **2**) gives the five double bonded 5,6-dihydro PSB11 (**4**). In other words, the retinal π-conjugation running from C5—NH^+ is first, extended to C3—NH^+ and second, aborted and then truncated to only C7—NH^+. Also, the 6-*s*-*trans* form of model **2** calculated to be 3.6 kcal·mol^{-1} less stable than the 6-*s*-*cis*-isomer in squid rhodopsin is included to complete the study (**5**). In the case of PSB11, 6-*s*-*cis* isomer is calculated to be ~10 kcal·mol^{-1} more stable than the 6-*s*-*trans* form in both squid and bovine rhodopsins and also in good agreement with theoretical findings on deep red cone pigments.9

The overall charge of the total system is +1, due to the PSB11-K305/K296 linkage. All atoms of the protein containing retinal analogues were fully optimized without any constraints using the hybrid QM/MM (QM=B3LYP/6-31G*; MM=AMBER96) method in

ONIOM (Our own *N*-layer Integrated molecular Orbital + molecular Mechanics) electronic embedding scheme implemented in Gaussian03.14

Ab initio multireference QM/MM calculations on the resulting structures at the spectroscopy oriented configuration interaction (SORCI+Q)/6-31G* level15 was applied using the ORCA 2.6.19 program package on top of the three-root (6e,6o) complete active space self-consistent field (CASSCF) wave functions to calculate the absorption and circular dichroism (CD) spectra in gas phase (QM) and in the protein (QM/MM). The vertical excitation energies as well as oscillator and rotatory strengths to first (S_1) and second (S_2) excited states were calculated for all of the structures discussed in this study. We estimate the accuracy of this computational setup to be 15 nm, and we showed previously that the present setup yielded results in excellent agreement with experimental measurements.4

As we enter into the protein environment, the most logical place to start the investigation is to look at the geometrical parameters of the chromophore (Figure 1) as a consequence of binding to the opsin. The details of the bond length alternation (BLA) pattern (Figure 1, bottom) of model **1** in both bovine and squid rhodopsins have been documented elsewhere.4 In the case of models **2** and **5**, extending the π-conjugation by one more double bond at C3=C4 reduces the ensuing C4—C5 single bond by 0.05 Å (1.51→1.46 Å). Aborting the conjugation by saturating the C5=C6 bond (**3**) bestows adequate flexibility to the retinal as evident in the dramatic increase of C5—C6 bond length to ~1.57 Å in both protein environments. Truncating the retinal to only five double bonds (**4**) eases the strain on the C4—C5 single bond and increases it by 0.04 Å (1.51→1.55 Å). Therefore, with respect to the BLA it is fair to suggest that, changes incorporated into the cyclic portion of the retinal seem to exert significant perturbation only on the neighboring single/double bonds and that the other half of retinal backbone essentially remain unperturbed. Apparently, both bovine and squid rhodopsin binding pockets consist of at least five aromatic residues within 4.0 Å environment of the β-ionone ring (Figure 2).3,4 Therefore, contact between the β-ionone ring and opsin through secondary hydrophobic interactions16 leading to retinal photoisomerization17 cannot be ruled out at this stage.

Perusal of the bond (Figure 1, middle) and dihedral (Figure 1, top) angle deviations also reveal the extensive perturbation the retinal has undergone starting from C3 to C8 (Figure 1, grey box). In particular, comparing models **3** and **4** provide an indirect evidence to the presence of weak H-bonding interaction at the Schiff base terminal in squid rhodopsin4 in agreement with FTIR studies.18 The dramatic change in the C6—C7 dihedral angle (from −45° in model **1** to −120° in models **3** and **4**) in conjunction with a slight displacement of the position of non-H-bonding counterion (E180) provides evidence for a flexible binding site in squid rhodopsin. On the contrary, little change in the C6—C7 dihedral angle between model **1** and models **3** and **4** coupled with an unaltered position of H-bonding counterion (E113) throughout the investigation (see supporting information) indicates a stiff binding site in the bovine rhodopsin. For models **1**, **2** and **5**, almost all the calculations yield a distorted C6—C7 single bond with torsional angle in the vicinity of −45° in good agreement with both the experimental19 and theoretical findings.20

Generally, the spectral tuning of dehydro and dihydro rhodopsins have been known to depend on the length of retinal conjugation.13 This property is evident in the calculated vertical excitation energy in both gas phase and protein environments which correlates well with the number of double bonds in PSB11 (Figure 3). Compared to the wild-type (**1**) that contains six-double bonds and absorb at 604/616 nm in gas phase and 490/495 nm in protein, model **2** contains seven-double bonds and absorb at 707/720 in gas phase and 510/534 nm in protein. However, model **3** also containing six-double bonds but with an aborted retinal conjugation (from C5 to C7) absorb at 532/510 nm in gas phase and 442/445

nm in protein. Model **4** that contains only five double bond also absorbs at 533/521 nm in gas phase and 459/447 nm in protein, thus supporting the hypothesis that model **3** may essentially behave as a five-double bonded retinal.6b

Model **5**, an isomer of model **2** also absorb at 727/708 nm in gas phase and 563/554 nm in protein. Therefore, increase/decrease in the retinal conjugation by one double bond separates the vertical excitation energy by ~100 nm in gas phase and ~60 nm in protein. As we turn off charges of the counterion (E180 in squid and E113 in bovine), the calculated vertical excitation energy in protein becomes almost on par with the gas phase (see w/o E180, w/o E113 in Figure 3). Therefore, similar to the native visual4,21 and archaeal22 rhodopsins, mechanism of spectral tuning in dehydro and dihydro rhodopsins are also steered by the strong electrostatic interaction between PSBR and counterion and the calculated results are also in good agreement with experimental findings on related rod visual pigments.6–8,13,23,24

Optical activity of rhodopsin is induced when retinal is bound to opsin. However, squid acid metarhodopsin does not show circular dichroism25 which suggests there are exceptions. Generally, out of plane distortion of the C11=C12 (negative) and C12—C13 (positive) bonds imparts a positive helicity on retinal yielding a positive rotatory strength (R).26 Surprisingly, magnitude of the calculated R of model **2** (+0.66 au) is almost double than model **1** (+0.32 au), while that of model **3** is almost equal (+0.33 au) to model **1** in squid rhodopsin. A relatively similar trend is also seen in the case of bovine rhodopsin (see supporting information).

In conclusion, dehydration and hydration of the β-ionone ring in both the squid and bovine rhodopsins are computationally studied for the first time. Our findings suggest that, i) modification of the retinal conjugation in β-ionone ring does not seem to affect the other half of the retinal backbone; ii) of all the retinal analogues considered, 3,4-de-5,6-dihydro and 5,6-dihydro retinals serve as more suitable probes to characterize the protein binding sites: the binding site of invertebrate squid rhodopsin as *malleable and ductile*, and that of vertebrate bovine rhodopsin as *rigid and stiff*; iii) the mechanism of spectral tuning in both dehydro and dihydro rhodopsins is steered by the strong electrostatic interaction between PSBR and the counterion; iv) twisting of the β-ionone ring relative to the polyene chain is almost irrelevant to the optical activity of visual pigments6b and finally, v) as the binding site of salamander rhodopsin containing model **2** remains unknown, our calculations incorporating model **2** into squid and bovine binding sites allows us to predict that, the same overall electrostatic and steric properties of the retinal structure are likely to exist for salamander as well. In other words, the red-shift of ~20 nm separating PSB11 in squid and/or bovine rhodopsin from that of 3,4-dehydro-PSB11 in salamander rhodopsin is essentially due to the extension of retinal π-conjugation and not due to any particular residue-based mechanism.

Supplementary Material

Refer to Web version on PubMed Central for supplementary material.

Acknowledgments

Authors would like to thank Dr. Tetsuji Okada at Gakushin University for valuable discussions during the course of this work. The work at Emory is supported in part by a grant from the National Institutes of Health (R01EY016400-04) and at Kyoto by a Core Research for Evolutional Science and Technology (CREST) grant in the Area of High Performance Computing for Multiscale and Multiphysics Phenomena JST.

References

1. a) Birge RR. Annu Rev Phys Chem. 1990; 41:683–733. [PubMed: 2257039] b) Kandori K, Shichida Y, Yoshizawa T. Biochemistry. 2001; 66:1197–1209. [PubMed: 11743865]
2. a) Terakita A, Yamashita T, Tachibanaki S, Shichida Y. FEBS Lett. 1998; 439:110–114. [PubMed: 9849889] b) Yokoyama S. Prog Ret Eye Res. 2000; 19:385.
3. a) Shimamura T, Hiraki K, Takahashi N, Hori T, Ago H, Masuda K, Takio K, Ishiguro M, Miyano M. J Biol Chem. 2008; 283:17753–17756. [PubMed: 18463093] b) Murakami M, Kouyama T. Nature. 2008; 453:363–367. [PubMed: 18480818]
4. a) Sekharan S, Altun A, Morokuma K. Chem Eur J. 2010; 16:1744–1749. b) Sekharan S, Morokuma K. J Phys, Chem Lett. 2010; 1:668–672. [PubMed: 20396622] c) Altun A, Yokoyama S, Morokuma K. J Phys Chem B. 2008; 112:16883–168890. [PubMed: 19367945] d) Altun A, Yokoyama S, Morokuma K. J Phys Chem A. 2009; 113:11685–11692. [PubMed: 19630373]
5. Dartnall HJ, Lythgoe JN. Vision Res. 1965; 5:81–100. [PubMed: 5862952]
6. a) Blatz PE, Dewhurst PB, Balasubramaniyan P, Balasubramaniyan V. Nature. 1968; 219:169–170. [PubMed: 5659644] b) Azuma M, Azuma K, Kito Y. Biochim Biophys Acta. 1973; 295:520–527. [PubMed: 4699576]
7. a) Cornwall M, Macnichol EF Jr, Fein A. Vision Res. 1984; 24:1651–1659. [PubMed: 6533990] b) Makino CL, Kraft TW, Mathies RA, Lugtenburg J, Miley ME, van der Steen, Baylor DA. J Physiol. 1990; 424:545–560. [PubMed: 2391661] c) Makino CL, Groesbeek M, Lugtenburg J, Baylor DA. Biophys J. 1999; 77:1024–1035. [PubMed: 10423447] d) Isayama T, Alexeev D, Makino CL, Washington I, Nakanishi K, Turro NJ. Nature. 2006; 443:649. [PubMed: 17035994]
8. Chen JG, Nakamura T, Ebrey TG, Ok H, Konno K, Derguini F, Nakanishi K, Honig B. Biophys J. 1989; 55:725–729. [PubMed: 2524224]
9. Amora TL, Ramos LS, Galan JF, Birge RR. Biochemistry. 2008; 47:4614–4620. [PubMed: 18370404]
10. Spudich JL, McCain DA, Nakanishi K, Okabe M, Shimizu N, Rodman H, Honig B, Bogomolni RA. Biophys J. 1986; 49:479–483. [PubMed: 2937462]
11. Lanyi JK, Zimanyi L, Nakanishi K, Derguini F, Okabe M, Honig. Biophys J. 1988; 53:185–191. [PubMed: 3345330]
12. DeGrip WJ, Bovee-Geurts PHM, van der Hoef I, Lugtenburg J. J Am Chem Soc. 2007; 129:13265–13269. [PubMed: 17918843]
13. Arnaboldi M, Motto MG, Tsujimoto K, Balogh-Nair V, Nakanishi K. J Am Chem Soc. 1979; 101:7082–7084.
14. Vreven T, Byun KS, Komaromi I, Dapprich S, Montgomery JA Jr, Morokuma K, Frisch MJ. J Chem Theory Comput. 2006; 2:815.
15. Neese FA. J Chem Phys. 2003; 119:9428–9443.
16. Matsumoto H, Yoshizawa T. Nature. 1975; 258:523–526. [PubMed: 1196384]
17. Ahuja S, Hornak V, Yan EC, Syrett N, Goncalves JA, Hirshfeld A, Ziliox M, Sakmar TP, Sheves M, Reeves PJ, Smith SO, Eilers M. Nat Struct Mol Biol. 2009; 16:168–175. [PubMed: 19182802]
18. Ota T, Furutani Y, Terakita A, Yoshinori S, Kandori H. Biochemistry. 2006; 45:2845–2851. [PubMed: 16503639]
19. Mollevanger LCPJ, Kentgens PM, Pardoen JA, Weeman WS, Lugtenburg J, DeGrip WJ. Eur J Biochem. 1987; 163:9–14. [PubMed: 3816805]
20. Honig B, Hudson B, Sykes BD, Karplus M. PNAS. 1971; 68:1289–1293. [PubMed: 5288377]
21. a) Gascon JA, Sproviero EM, Batista VS. Acc Chem Res. 2006; 39:184–193. [PubMed: 16548507] b) Sekharan S, Sugihara M, Buss V. Angew Chem Int Ed Engl. 2007; 46:269–271. [PubMed: 17120281] c) Altun A, Yokoyama S, Morokuma S. J Phys Chem B. 2008; 112:6814–6827. [PubMed: 18473437]
22. a) Wanko M, Hoffmann, Wanko M, Strodel P, Kosolowski A, Thiel W, Neese F, Frauhenheim T, Elstner M. J Phys Chem B. 2005; 109:3606–3615. [PubMed: 16851399] b) Hoffmann M, Wanko M, Strodel P, König PH, Frauenheim T, Schulten K, Thiel W, Tajkhorshid E, Elstner M. J Am Chem Soc. 2006; 128:10808–10818. [PubMed: 16910676]

23. Koutalos Y, Ebrey TG, Tsuda M, Odashima K, Lien T, Park MH, Shimizu N, Derguini F, Nakanishi K, Gilson HR, Honig B. Biochemistry. 1989; 28:2732–2739. [PubMed: 2525050]
24. Sheves M, Nakanishi K. J Am Chem Soc. 1983; 105:4033–4039.
25. Kito Y, Azuma M, Maeda Y. Biochim Biophys Acta. 1968; 154:352–359. [PubMed: 5637054]
26. Shichida S, Tokunaga F, Yoshizawa T. Biochim Biophys Acta Bioenerg. 1978; 504:413–430.

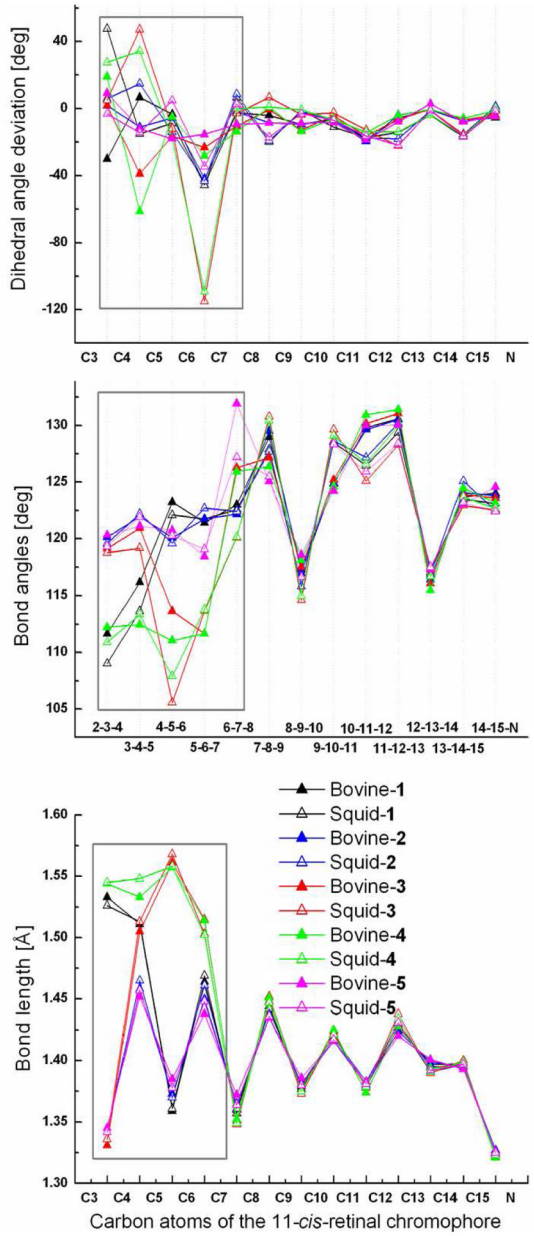

Figure 1.

Comparison of the bond length alternation (bottom), bond angles (middle) and dihedral angles (top) along the conjugated carbon chain of the optimized QM/MM geometries of PSB11 and analogues shown in Scheme 1. Unfilled/filled triangles denote the PSB11 models optimized in squid/bovine rhodopsin. The grey colored box indicates the region that has undergone maximum perturbation along the length of the retinal chromophore. The dihedral angle deviations are from either *cis* (0°) or *trans* (180°) configuration.

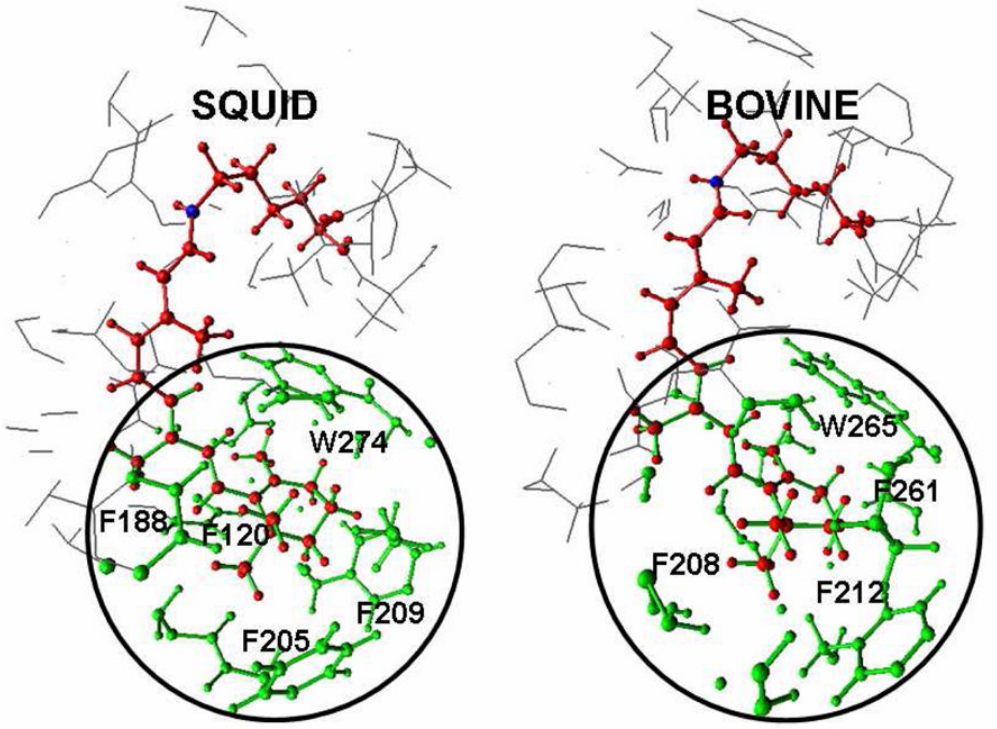

Figure 2.
Comparison of the squid (left hand side) and bovine (right hand side) rhodopsin binding pockets. Residues within 4 Å environment of any atom in PSB11 are shown in grey (lines). Black circle indicate the residues (shown in green colored ball and stick model) within 4 Å environment of any atom in the β-ionone portion of PSB11.

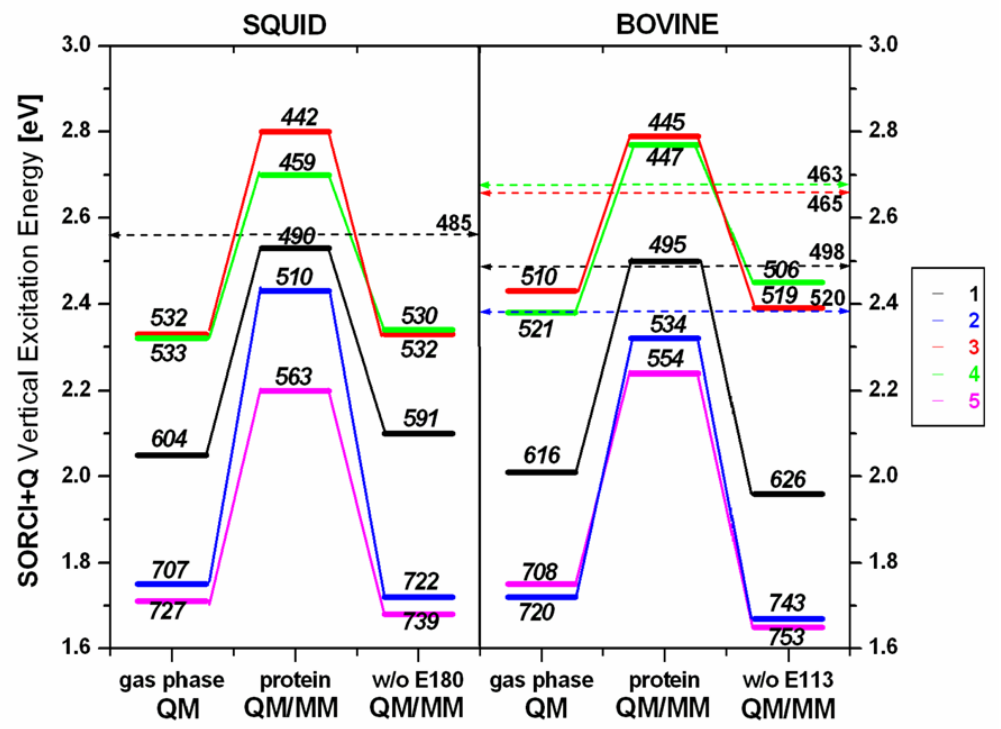

Figure 3.

SORCI+Q calculated $S_1 \rightarrow S_0$ vertical excitation energies in eV (wavelength in nm) of the PSB11 analogues in gas phase (**QM**) and protein (**QM/MM**) environments of squid and bovine rhodopsin. Calculations involving the protein environment without charges of its counterion (**w/o E180, w/o E113**) are also plotted. Color code: black–**1**, blue–**2**, red–**3**, green–**4**, magenta–**5** for PSB11 models depicted in Scheme 1. Horizontal dashed lines on the left (squid) and right (bovine) hand side indicate the corresponding experimental values taken from refs. 6, 7, 23–26. The calculated $S_2 \rightarrow S_0$ values of all the PSB11 analogues discussed in this study are given in the supporting information.

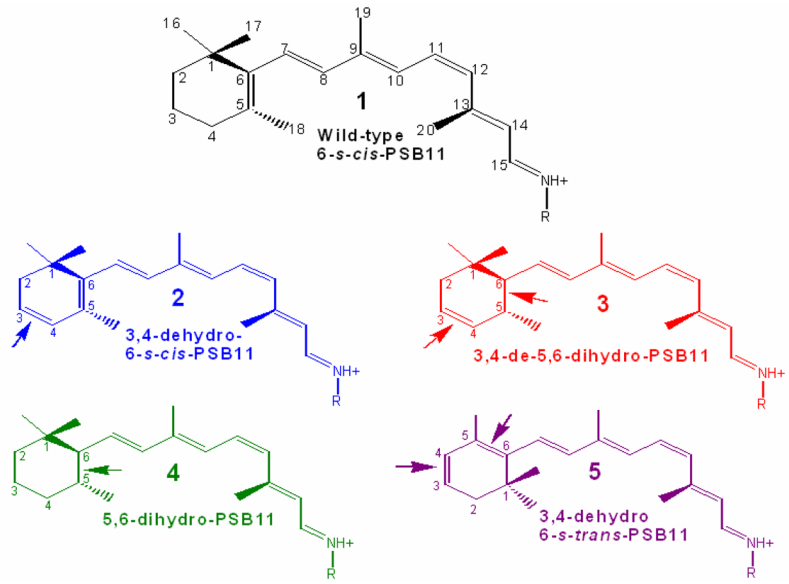

Scheme 1.

Schematic representation of the structures of wildtype, dehydro- and dihydro- protonated Schiff base of 11-*cis*-retinal chromophores incorporated into squid and bovine rhodopsins. R-refers to K305/K296 in their respective protein environments. The arrow points to the location at which the retinal is modified.